

Article

Impact of Warm Dark Matter on the Cosmic Neutrino Background Anisotropies

Christopher G. Tully^{1,*}  and Gemma Zhang² ¹ Department of Physics, Princeton University, Princeton, NJ 08544, USA² Department of Physics, Harvard University, Cambridge, MA 02138, USA; yzhang7@g.harvard.edu

* Correspondence: cgtully@princeton.edu

Abstract: The Cosmic Neutrino Background (C ν B) anisotropies for massive neutrinos are a unique probe of large-scale structure formation. The redshift-distance measure is completely different for massive neutrinos as compared to electromagnetic radiation. The C ν B anisotropies in massive neutrinos grow in response to non-relativistic motion in gravitational potentials seeded by relatively high k -modes. Differences in the early phases of large-scale structure formation in warm dark matter (WDM) versus cold dark matter (CDM) cosmologies have an impact on the magnitude of the C ν B anisotropies for contributions to the angular power spectrum that peak at high k -modes. We take the examples of WDM consisting of 2, 3, or 7 keV sterile neutrinos and show that the C ν B anisotropies for 0.05 eV neutrinos drop off at high- l multipole moment in the angular power spectrum relative to CDM. At the same angular scales that one can observe baryonic acoustical oscillations in the CMB, the C ν B anisotropies begin to become sensitive to differences in WDM and CDM cosmologies. The precision measurement of high- l multipoles in the C ν B neutrino sky map is a potential possibility for the PTOLEMY experiment with thin film targets of spin-polarized atomic tritium superfluid that exhibit significant quantum liquid amplification for non-relativistic relic neutrino capture.

Keywords: warm dark matter (WDM); cosmic neutrino background (CNB); large-scale structure (LSS); PTOLEMY; relic neutrinos; spin-polarized atomic tritium; superfluid; quantum liquid amplification; relic neutrino capture



Citation: Tully, C.G.; Zhang, G. Impact of Warm Dark Matter on the Cosmic Neutrino Background Anisotropies. *Universe* **2022**, *8*, 118. <https://doi.org/10.3390/universe8020118>

Academic Editor: Norma G. Sanchez

Received: 4 January 2022

Accepted: 10 February 2022

Published: 12 February 2022

Publisher's Note: MDPI stays neutral with regard to jurisdictional claims in published maps and institutional affiliations.



Copyright: © 2022 by the authors. Licensee MDPI, Basel, Switzerland. This article is an open access article distributed under the terms and conditions of the Creative Commons Attribution (CC BY) license (<https://creativecommons.org/licenses/by/4.0/>).

1. Introduction

The “null assumption” of the cosmological principle is that the universe on large scales is homogeneous and isotropic. Deviations from this assumption are, therefore, a measure of large-scale structure formation. Perhaps one of the most salient anisotropies appears in the Cosmic Microwave Background (CMB) and through a detailed modeling of the early universe tells us the fraction of baryonic matter to the total matter in the universe. The baryonic matter is distinguished from the total matter through the formation of sound waves in a relativistic plasma before the period of plasma recombination [1]. The nature of the non-plasma/dark matter is largely unknown with an important exception being the fraction of neutrinos which are predicted from the Cosmic Neutrino Background (C ν B). Anisotropies in the C ν B massive neutrinos are also an important measure of large-scale structure formation and reveal an earlier period of dynamics than viewed at equivalent distances using optical probes.

As described in Ref. [2], the C ν B anisotropies for massive neutrinos grow rapidly during the non-relativistic phase of their motion. With directionality, as proposed by the PTOLEMY experiment with a polarized tritium target, the C ν B neutrino capture rate variation provides a map of the anisotropies on the neutrino sky as seen on Earth. The variations on the neutrino sky are, therefore, a measure of the total matter power spectrum at redshifts relevant to C ν B anisotropy growth. Depending on the model for dark matter, the total matter power spectrum can differ during the period of C ν B anisotropy growth. In particular,

warm dark matter consisting of 2–7 keV sterile neutrinos has a different contribution to the CνB anisotropies as compared to cold dark matter. Cold dark matter is assumed to have exactly zero pressure at high redshift while warm dark matter carries some degree of non-zero radiation pressure according to its mass [3,4].

2. CνB Angular Power Spectra

The total matter linear power spectra are shown in Figure 1 with the WDM modeled as a 2 keV sterile neutrino in addition to a normal mass hierarchy of active neutrinos, the lightest massless, and computed using the CLASS software implemented within CONCEPT [5,6]. The CDM is modeled with the same normal mass hierarchy of active neutrinos. At a redshift of $z = 1$, the warm and cold dark matter models predict a different amount of linear power for k -modes of approximately 1 Mpc^{-1} and higher. The differences in WDM and CDM in the high k -modes become less distinct at low redshift under the effects of non-linear dynamics [7]. The redshifts relevant to the CνB anisotropies for neutrinos with a mass of 0.05 eV are shown in Figure 2. The bulk of the fractional contribution to the total CνB angular power spectra for a neutrino mass of 0.05 eV come from redshifts of $z = 1$ and higher. The ratio of the CνB angular power spectra for CDM and WDM with a 2, 3, or 7 keV sterile neutrino is shown in Figure 3. Differences can be seen in the high- l modes.

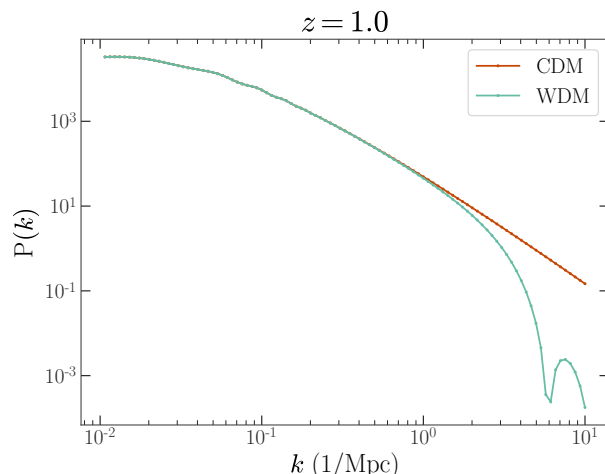


Figure 1. The total matter linear power spectra for CDM and WDM with a 2 keV sterile neutrino.

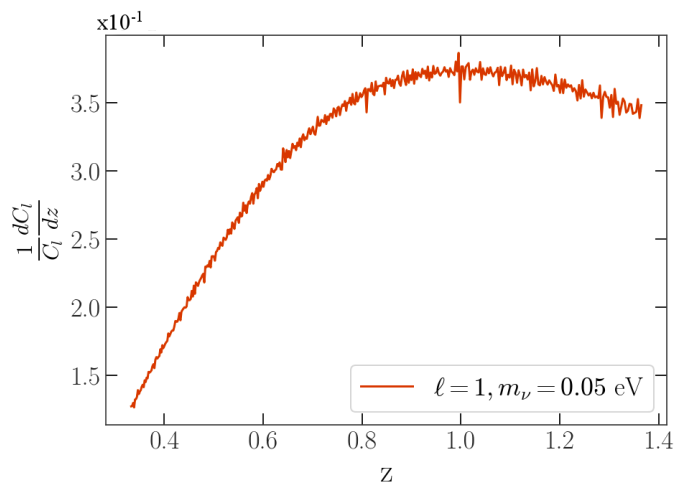


Figure 2. The fractional contribution to the $l = 1$ multipole of the CνB angular power spectrum for a neutrino mass of 0.05 eV as a function of redshift.

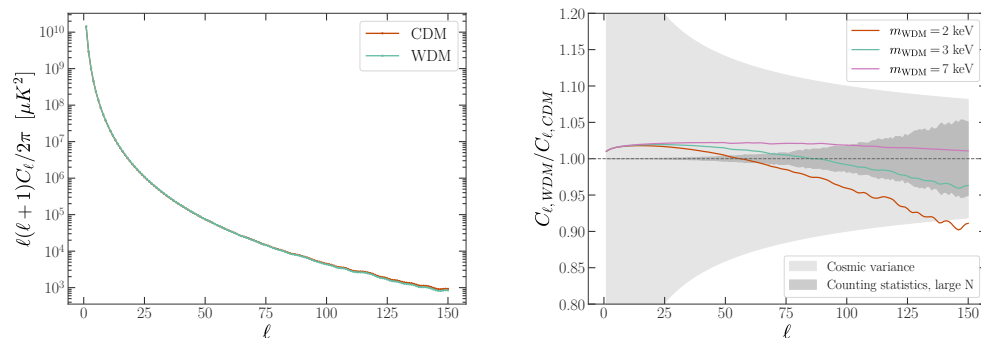


Figure 3. (left) The total CνB angular power spectra for CDM and WDM with a 2 keV sterile neutrino. (right) The ratio of the CνB angular power spectra for CDM and WDM cosmologies for a sterile neutrino mass of 2, 3, or 7 keV. The impact of WDM is a relative drop in the CνB angular power at high-*l*. The contributions to the total uncertainty on the measurement of the ratio are shown for cosmic variance and the PTOLEMY counting statistics in the limit of large-*N* total neutrino capture events.

The total uncertainty on the measurement of the CνB angular power spectrum has contributions from cosmic variance and the PTOLEMY counting statistics for the total number of neutrino capture events. The fractional one-standard-deviation uncertainty on C_ℓ from cosmic variance is given by

$$\frac{\Delta C_\ell}{C_\ell} = \sqrt{\frac{2}{2l + 1}} \quad (\text{cosmic variance}) \tag{1}$$

where for $l = 150$, the fractional uncertainty is 8.2% [8]. The fractional uncertainty on the measurement of C_ℓ from the PTOLEMY counting statistics per *l*-mode was determined numerically. The procedure was to generate a temperature map, as in Ref. [2], and to interpret the map as a count rate map for neutrino captures, without folding in the angular smearing from the polarized tritium target. The expected count per pixel on the sky is then smeared using Poisson statistics. The map is then inverted to find the C_ℓ and this procedure is repeated for several trials. We verified that the fractional uncertainty on C_ℓ agrees with the expected $1/\sqrt{N}$ behavior for *N* neutrino capture events. For a full data analysis, not part of this study, one would minimize the number of total bins on the sky map, the total counting statistics for a given highest-*l* and include angular folding and unfolding studies for neutrino capture events.

The contributions of cosmic variance and counting statistics to the fractional uncertainties on C_ℓ are shown in Figure 3 and compared to the expected effects from WDM. The rapid growth of the counting statistics uncertainties for high-*l* has a direct impact on the measurement of WDM effects. The total number of neutrino captures is nominally limited by the target nuclei capture cross section, CνB flux and density of states, the total number of nuclei in the target and the acceptance efficiency of the PTOLEMY spectrometer. However, it may be possible to bring down the counting statistics uncertainties to a level where the WDM effects can be observed in the data, under the linear assumptions made here, with an amplification mechanism, as described in the following section. Further investigations on the C_ℓ predictions including the non-linear matter power spectra are needed.

3. Quantum Amplification of Neutrino Capture

The possibility of a superfluid ground-state condensate of spin-polarized tritium atoms may provide an amplification mechanism for the process of relic neutrino capture. Spin-polarized tritium atoms, which are neutral bosons, have long been considered an ideal candidate to form a quantum liquid [9]. The lightest spin-polarized hydrogen isotope in a gaseous phase was successfully cooled down in a magnetic trap to form a Bose–Einstein Condensate in 1998 [10]. The heavier mass of the tritium reduces the zero-point motion and

opens up the possibility of forming a liquid a low temperatures. Thin films of superfluid spin-polarized tritium adsorbed onto the surface of superfluid ${}^4\text{He}$ may be a suitable target for the PTOLEMY experiment that aims to detect and measure the anisotropies of the $C_{\nu B}$ [11,12].

The mechanism for quantum liquid amplification of relic neutrino capture is shown diagrammatically in Figure 4 and compared to the more familiar process of a laser. In a laser, the long time-constant for the decay of an electron in an excited state of atom A^* is dramatically shortened by the proximity of a photon condensate that shares a final state momentum available to a photon emitted in the de-excitation process of the atomic state. For a photon emitted into the condensate, the amplitudes for all possible exchange diagrams add with a positive sign for Bose–Einstein statistics and effectively create an amplification of $N + 1$ for the de-excitation process in the presence of N indistinguishable photons. Any process that stimulates the de-excitation or cooling of a non-condensate spin-polarized tritium atom T_{\downarrow}^* so that it falls into the ground-state T_{\downarrow} condensate will be amplified in a similar manner.

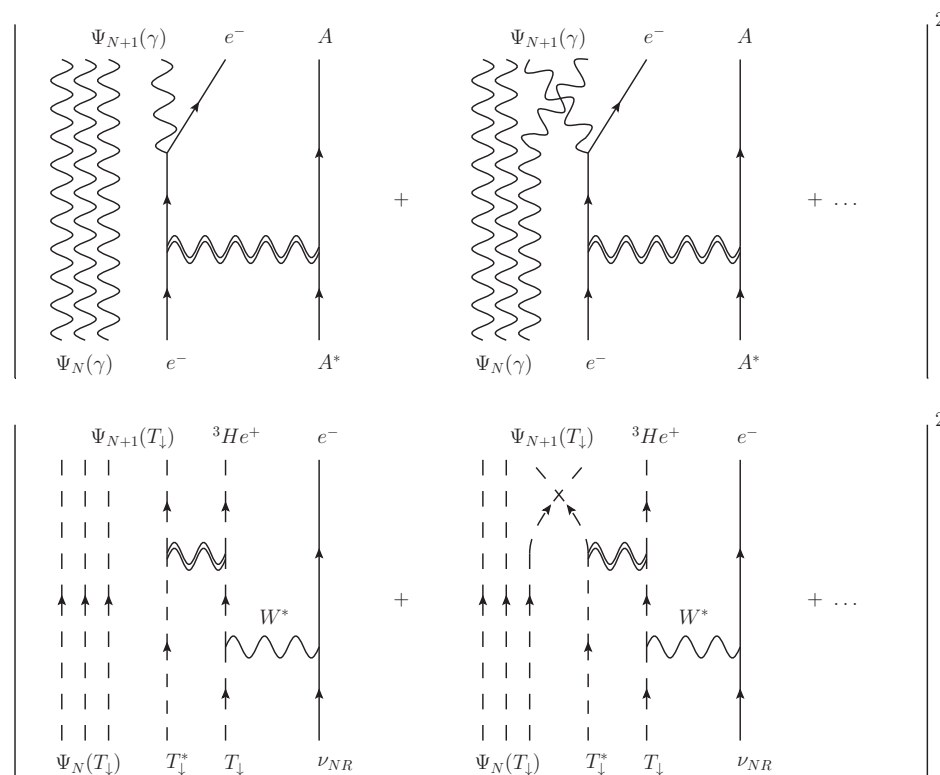


Figure 4. Comparison of a laser (top) to a quantum liquid amplification process for relic neutrino capture (bottom). The amplitudes for exchange terms involving the stimulated increase from N to $N + 1$ bosons in the final-state condensate sum coherently with a positive sign following Bose–Einstein statistics.

The processes of relic neutrino capture and tritium β -decay produce an electron and a ${}^3\text{He}^+$ ion in the final state, with the addition of an anti-neutrino for β -decay. The ${}^3\text{He}^+$ ion, in particular, has an attractive potential energy with atomic tritium and the ejection of the ${}^3\text{He}^+$ ion from a spin-polarized tritium superfluid has to the potential to provide a cooling mechanism for non-condensate spin-polarized tritium atoms. A two-fluid model for the tritium superfluid would naturally provide an admixture of ground-state condensate and non-condensate atoms in the liquid phase [13,14]. The coherence length of the superfluid sets the average number N of atoms in a cluster of ground-state condensate. For each spectator T_{\downarrow}^* that de-excites into a ground-state cluster, there are $N + 1$ coherent amplitudes contributing to the final state. For symmetric heating/cooling probabilities of the ${}^3\text{He}^+$ ion

interacting with the tritium superfluid, one would want more normal than ground-state condensate fraction to have a population inversion. For the case of relic neutrino capture, the similarity of the process with tritium β -decay would allow the amplification factor to be determined directly from the shortening of the lifetime of spin-polarized tritium atoms in the superfluid.

The wavelengths of relic neutrinos are macroscopic. The typical momentum of a relic neutrino averaged over the density of states of a relativistic Fermi–Dirac distribution is roughly $p_\nu = 3k_B T_\nu/c \approx 0.5 \text{ meV}/c$. The corresponding de Broglie wavelength is $\lambda_\nu = h/p_\nu \approx 3 \text{ mm}$. Although the wavelength of the relic neutrino does not directly factor into the cooldown of non-condensate, spectator spin-polarized tritium atoms (coherent neutral current scattering is suppressed by the weak interaction), the probability of a T_\downarrow^* spectator to be within λ_ν is high.

The formation of thin films of superfluid spin-polarized tritium atoms has not been achieved experimentally, though one can consider experimental constraints on these systems for use in the PTOLEMY experiment. For a liquid density (atoms/volume) of 0.008 \AA^{-3} , the thickness of the films should be limited to roughly 500 \AA , equivalent to roughly 100 layers of hydrogen. At this thickness, the Poisson probability for tritium endpoint electrons to inelastically scatter before exiting the thin film target is small [15,16]. The recombination rate and the heating effects of tritium β -decay should have a limited impact on the active target performance with a suitable active target liquid recirculating procedure. Recycling of the superfluid target is needed to regenerate stable operating conditions. Similarly with the previous constraint, the vacuum above the thin film should be maintained and pumped down to prevent target materials from entering the spectrometer vacuum regions. Though there are no estimates for the coherence lengths for a spin-polarized tritium superfluid, the coherence length in a 3D liquid up to the thickness of the film could provide as large as $N = (10^2)^3$ atoms in the condensate clusters increasing the equivalent target mass significantly. The nominal PTOLEMY $C\nu B$ detection rate for 100 g of tritium is 10 events per year, much fewer than needed to measure even the $l = 1$ dipole moment. A significant gain factor on the neutrino capture rate would open up the possibility for more detailed studies of the $C\nu B$ anisotropies. Figure 3 shows the importance of reducing the uncertainty from counting statistics on the measurement of high l -modes in order to measure the effects of WDM.

The quantum amplification of relic neutrino capture, if this possibility can be realized in physical systems, opens up an exciting possibility for precision measurements of the $C\nu B$ anisotropies out to high multipole moments in the angular power spectrum.

4. Results and Conclusions

At the same angular scales that one can observe baryonic acoustical oscillations in the CMB, the $C\nu B$ anisotropies start to become sensitive to differences in WDM and CDM cosmologies. Within the limitations of linear power spectra, deviations of the angular power spectra for $C\nu B$ show sensitivity to the downward trend in the expected C_ℓ toward high- l for sterile neutrino masses of 2 and 3 keV. Heavier masses of 7 keV are comparable to the CDM. The cosmic variance uncertainties impose a limitation on the expected fluctuations in C_ℓ , but it may be possible to reduce these effects for the $C\nu B$ using the multi-messenger approach described in Ref. [2]. By correlating $C\nu B$ anisotropies to luminous tracers that track the matter power spectrum, cosmic variance can be replaced by data-derived predictions for the $C\nu B$ anisotropies using optical data. Extensive galactic surveys, such as SDSS IV/V, track baryonic matter and can be used to provide a more direct handle on the onset of non-linear power effects at low redshift [17].

The quantum liquid amplification process described here for enhancing relic neutrino capture increases the effective tritium target mass for a fixed area and a given time exposure with the possibility to provide sufficient counting statistics needed to observe the impact of WDM on the $C\nu B$ anisotropies. The quantum liquid amplification process, if it can be realized in a practical configuration, may also be relevant for limited aperture MAC-E

neutrino mass experiments and direct keV-mass sterile neutrino searches that look for kinematic thresholds appearing in the tritium spectrum [18,19]. Effects of mixing may open up the possibility of direct sterile neutrino capture [20]. The superfluid tritium target as a highly delocalized state of atomic tritium also has the potential to reduce zero-point motion effects on the tritium endpoint electron energy distribution [21,22].

Author Contributions: C.G.T. and G.Z. worked jointly on all aspects of Angular Power Spectra. C.G.T. worked on all aspects of Quantum Amplification. All authors have read and agreed to the published version of the manuscript.

Funding: CGT is supported by the Simons Foundation grant number 377485.

Informed Consent Statement: Not applicable .

Data Availability Statement: The code used to compute the figures shown in this paper was accessed on 7 November 2021 at <https://github.com/gemyxzhang/cnb-anisotropies>.

Acknowledgments: A deep gratitude to Hector de Vega and Norma Sanchez for their early acknowledgement in 2013 of the future potential of the PTOLEMY experiment and the discussions and interactions that contributed to this work as part of the Ecole Chalonge-deVega.

Conflicts of Interest: The authors declare no conflict of interest.

References

- Kamionkowski, M.; Kosowsky, A. The cosmic microwave background and particle physics. *Annu. Rev. Nucl. Part. Sci.* **1999**, *49*, 77–123. [[CrossRef](#)]
- Tully, C.G.; Zhang, G. Multi-messenger astrophysics with the cosmic neutrino background. *J. Cosmol. Astropart. Phys.* **2021**, *6*, 053. [[CrossRef](#)]
- de Vega, H.J.; Sanchez, N.G. Equation of state, universal profiles, scaling and macroscopic quantum effects in warm dark matter galaxies. *Eur. Phys. J. C* **2017**, *77*, 1–19. [[CrossRef](#)]
- Hipólito-Ricaldi, W.S.; vom Marttens, R.; Fabris, J.; Shapiro, I.; Casarini, L. On general features of warm dark matter with reduced relativistic gas. *Eur. Phys. J. C* **2018**, *78*, 1–13. [[CrossRef](#)]
- Blas, D.; Lesgourgues, J.; Tram, T. The Cosmic Linear Anisotropy Solving System (CLASS). Part II: Approximation schemes. *J. Cosmol. Astropart. Phys.* **2011**, *2011*, 034. [[CrossRef](#)]
- Dakin, J.; Brandbyge, J.; Hannestad, S.; Haugbølle, T.; Tram, T. CONCEPT: Cosmological neutrino simulations from the non-linear Boltzmann hierarchy. *J. Cosmol. Astropart. Phys.* **2019**, *2019*, 052. [[CrossRef](#)]
- Viel, M.; Markovič, K.; Baldi, M.; Weller, J. The non-linear matter power spectrum in warm dark matter cosmologies. *Mon. Not. R. Astron. Soc.* **2012**, *421*, 50–62. [[CrossRef](#)]
- Peebles, P.J.E. *The Large-Scale Structure of the Universe*; Princeton University Press: Princeton, NJ, USA, 1980; p. 435.
- Bešlić, I.; Vranješ Markić, L.; Boronat, J. Spin-polarized hydrogen and its isotopes: A rich class of quantum phases. *Low Temp. Phys.* **2013**, *39*, 857–873. [[CrossRef](#)]
- Fried, D.G.; Killian, T.C.; Willmann, L.; Landhuis, D.; Moss, S.C.; Kleppner, D.; Greytak, T.J. Bose-Einstein condensation of atomic hydrogen. *Phys. Rev. Lett.* **1998**, *81*, 3811. [[CrossRef](#)]
- Marín, J.; Markić, L.V.; Boronat, J. Spin-polarized hydrogen adsorbed on the surface of superfluid ^4He . *J. Chem. Phys.* **2013**, *139*, 224708. [[CrossRef](#)]
- Betti, M.; Biasotti, M.; Boscá, A.; Calle, F.; Carabe-Lopez, J.; Cavoto, G.; Chang, C.; Chung, W.; Cocco, A.; Colijn, A.; et al. A design for an electromagnetic filter for precision energy measurements at the tritium endpoint. *Prog. Part. Nucl. Phys.* **2019**, *106*, 120–131. [[CrossRef](#)]
- London, H. Thermodynamics of the thermomechanical effect of liquid He II. *Proc. R. Soc. Lond. Ser. A. Math. Phys. Sci.* **1939**, *171*, 484–496.
- Landau, L. Theory of the superfluidity of helium II. *Phys. Rev.* **1941**, *60*, 356. [[CrossRef](#)]
- Aseev, V.; Belesev, A.; Berlev, A.; Geraskin, E.; Kazachenko, O.; Kuznetsov, Y.E.; Lobashev, V.; Ostroumov, R.; Titov, N.; Zadorozhny, S.; et al. Energy loss of 18 keV electrons in gaseous T and quench condensed D films. *Eur. Phys. J.-At. Mol. Opt. Plasma Phys.* **2000**, *10*, 39–52. [[CrossRef](#)]
- Abdurashitov, D.; Belesev, A.; Chernov, V.; Geraskin, E.; Golubev, A.; Koroteev, G.; Likhovid, N.; Nozik, A.; Pantuev, V.; Parfenov, V.; et al. Electron scattering on hydrogen and deuterium molecules at 14–25 keV by the “Troitsk nu-mass” experiment. *Phys. Part. Nucl. Lett.* **2017**, *14*, 892–899. [[CrossRef](#)]
- Kollmeier, J.A.; Zasowski, G.; Rix, H.W.; Johns, M.; Anderson, S.F.; Drory, N.; Johnson, J.A.; Pogge, R.W.; Bird, J.C.; Blanc, G.A.; et al. SDSS-V: Pioneering panoptic spectroscopy. *arXiv* **2017**, arXiv:1711.03234.
- Aker, M.; Beglarian, A.; Behrens, J.; Berlev, A.; Besserer, U.; Bieringer, B.; Block, F.; Bornschein, B.; Bornschein, L.; Böttcher, M.; et al. First direct neutrino-mass measurement with sub-eV sensitivity. *arXiv* **2021**, arXiv:2105.08533.

19. Mertens, S.; Brunst, T.; Korzeczek, M.; Lebert, M.; Siegmann, D.; Alborini, A.; Altenmüller, K.; Biassoni, M.; Bombelli, L.; Carminati, M.; et al. Characterization of silicon drift detectors with electrons for the TRISTAN project. *J. Phys. G Nucl. Part. Phys.* **2020**, *48*, 015008. [[CrossRef](#)]
20. Li, Y.F.; Xing, Z.Z. Possible capture of keV sterile neutrino dark matter on radioactive β -decaying nuclei. *Phys. Lett. B* **2011**, *695*, 205–210. [[CrossRef](#)]
21. Cheipesh, Y.; Cheianov, V.; Boyarsky, A. Heisenberg's uncertainty as a limiting factor for neutrino mass detection in β -decay. *arXiv* **2021**, arXiv:2101.10069.
22. Nussinov, S.; Nussinov, Z. Quantum Induced Broadening-A Challenge For Cosmic Neutrino Background Discovery. *arXiv* **2021**, arXiv:2108.03695.